DOI: http://dx.doi.org/10.22104/jpst.2015.178 Journal of Particle Science and Technology (2015) 141-151

Journal of Particle Science and Technology

J | P | S | T

jpst.irost.ir

# MHD Three-Dimensional Stagnation-Point Flow and Heat Transfer of a Nanofluid over a Stretching Sheet

**Aboutaleb Ghadami Jadval Ghadam[1,*], Abed Moradi [2]**

[1]*Department of Chemical Engineering, Yasouj Branch, Islamic Azad University, Yasouj, Iran*

[2]*Young Researchers Club, Yasouj Branch, Islamic Azad University, Yasouj, Iran*

## HIGHLIGHTS

- Three-dimensional magnetohydrodynamic (MHD) boundary layer of stagnation-point flow in a nanofluid was investigated.
- The similarity equations were solved for three types of nanoparticles (copper, alumina and titania) with water as the base fluid.
- Effects of solid volume fraction on flow and heat transfer characteristics were thoroughly examined.
- The skin-friction coefficient and Nusselt number as well as the velocity and temperature profiles for some values of the governing parameters were presented

## GRAPHICAL ABSTRACT

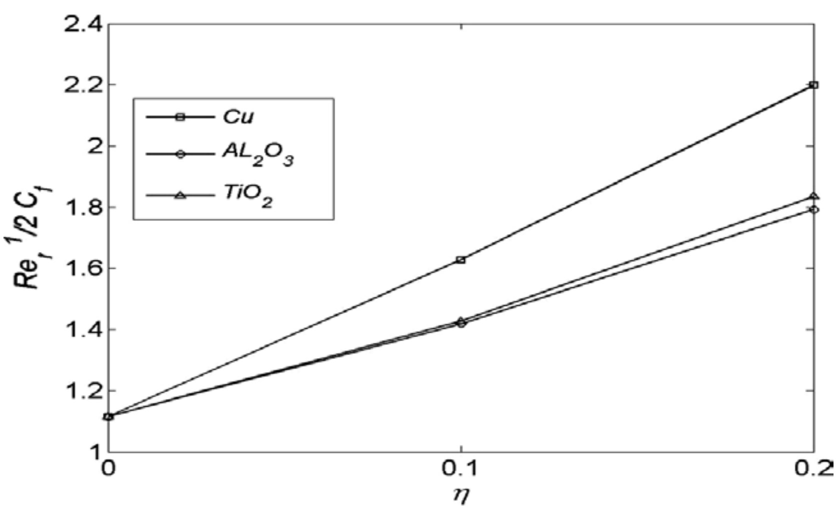


## ARTICLE INFO

*Article history:*
Received 5 October 2015
Received in revised form
2 November 2015
Accepted 12 November 2015

*Keywords:*
Nanofluid
Nanoparticles
Stagnation-point flow
MHD
Stretching plate

## ABSTRACT

In this study, the three-dimensional magnetohydrodynamic (MHD) boundary layer of stagnation-point flow in a nanofluid was investigated. The Navier–Stokes equations were reduced to a set of nonlinear ordinary differential equations using a similarity transform. The similarity equations were solved for three types of nanoparticles: copper, alumina and titania with water as the base fluid, to investigate the effect of the nanoparticle volume fraction parameter ($\phi$), the magnetic parameter ($M$), the Prandtl number ($Pr$) and the velocity ratio parameter ($\varepsilon$) on the flow and heat transfer characteristics. The skin-friction coefficient and Nusselt number as well as the velocity and temperature profiles for some values of the governing parameters were presented graphically and discussed. Effects of the solid volume fraction on the flow and heat transfer characteristics were thoroughly examined. It was observed that, for all three nonoparticles, the magnitude of the skin friction coefficient and local Nusselt number increased with enhancement in the nanoparticle volume fraction ($\phi$). In addition, the velocity of fluid increases by increasing $M$ and $\varepsilon$ and the temperature increases by decreasing $M$, $\varepsilon$ and $Pr$. The highest values of the skin friction coefficient and the local Nusselt number were obtained for the Cu nanoparticles compared to $Al_2O_3$ and $TiO_2$.

*Corresponding author. Tel: +989171458176

*E-mail address: aghadami80@gmail.com; ghadami@iauyasooj.ac.ir.*

## 1. Introduction

Stagnation-point flow, describing the fluid motion near the stagnation region of a solid surface exists in both cases of a fixed or moving body in a fluid. In the stagnation region, pressure is at its maximum value and the highest rate of heat transfer and mass deposition occurs. Hiemenz (1911) was the first to study the two-dimensional stagnation point flow, and obtained an exact similarity solution of the governing Navier–Stokes equations [1]. The axisymmetric three-dimensional stagnation point flow was studied by Homann, 1936 [2]. He demonstrated that the Navier-Stokes equations governing of the flow can be reduced to an ordinary differential equation of third order using similarity trans- formation. The results of these studies are of great technical importance, for example in the prediction of skin-friction as well as heat/mass transfer near stagnation regions of bodies in high speed flows and also in the design of thrust bearings and radial diffusers, drag reduction, transpiration cooling and thermal oil recovery. In 1942, Eckert [3] extended this work by including the energy equation and obtained an exact similar solution for the thermal field. In recent years, Dinarvand (2010) considered the off-centered stagnation flow towards a rotating disc by means of HAM [4]. It may be said that many investigators have considered various aspects of such flow and obtained closed form analytical as well as numerical solutions. The study of magnetohydrodynamic viscous flows has important industrial, technological and geothermal applications such as high-temperature plasmas, cooling of nuclear reactors, liquid metal fluids, MHD accelerators, and power generation systems. Duwairi and Damseh (2004) studied the radiation–conduction interaction in free and mixed convection fluid flow for a vertical flat plate in the presence of a magnetic field effect [5, 6]. Ece (2005) investigated the similarity analysis for the laminar free convection boundary layer flow in the presence of a transverse magnetic field over a vertical down-pointing cone with mixed thermal boundary conditions [7]. He determined the boundary layer velocity and temperature profiles numerically for various values of the magnetic parameter and the Prandtl number. Dinarvand et al., (2010) examined the unsteady laminar MHD flow near forward stagnation point of an impulsively rotating and translating sphere in presence of buoyancy forces [8]. Also, he studied the boundary-layer flow about a heated and rotating down-pointing vertical cone in the presence of a transverse magnetic field [9]. A nanofluid is a new class of heat transfer fluids that contains a base fluid and nanoparticles. The use of additives is a technique applied to enhance the heat transfer performance of base fluids. The thermal conductivity of the ordinary heat transfer fluids is not adequate to meet today's cooling rate requirements. Nanofluids have been shown to increase the thermal conductivity and convective heat transfer performance of the base liquids. In 1995, Choi seems to be the first who used the term nanofluids to refer to the fluid with suspended nanoparticles [10]. Choi, et al., (2001) showed that the addition of a small amount (less than 1% by volume) of nanoparticles to conventional heat transfer liquids increased the thermal conductivity of the fluid up to approximately two times [11]. One of the possible mechanisms for anomalous increasing in the thermal conductivity of nanofluids is the Brownian motions of the nanoparticles inside the base fluids. A variety of nuclear reactor designs featured by enhanced safety and improved economics are being proposed by the nuclear power industry around the world to more realistically solve the future energy supply shortfall. Nanofluid coolants show an improved thermal performance are being considered as a new key technology to secure nuclear safety and economics. Nanofluids are suspensions of nanoparticles in fluids that show significant enhancement of their properties at modest nanoparticle concentrations. Many of the publications on nanofluids are about understanding their behavior, so that they can be utilized where straight heat transfer enhancement is paramount as in many industrial applications such as: nuclear reactors, transportation, electronics as well as biomedicine and food. Magnetic nanofluid is a unique material that has both the liquid and magnetic properties. Many of the physical properties of these fluids can be turned by varying magnetic field. In addition, they have been wonderful model system for fundamental studies. As the magnetic nanofluids are easy to manipulate with an external magnetic field, they have been used for a variety of studies. Brownian diffusion and thermophoresis are important slip mechanisms in nanofluids. Many researchers have investigated different aspects of nanofluids. Thermophysical properties of nanofluids such as thermal conductivity, thermal diffusivity, and viscosity of nanofluids have been studied by literatures [12-18]. Ahmad and Pop [19] examined the mixed convection boundary layer flow past a vertical flat plate embedded in a porous medium filled with nanofluids. Mixed convective boundary layer flow of a nanofluid over a vertical circular cylinder has been studied by Dinarvand et al., 2015 [20]. The two-dimensional boundary layer flow of a nanofluid past a stretching sheet in the presence of magnetic field intensity and the thermal radiation was studied by Gbadeyan and Olanrewaju [21]. Dinarvand, et al., (2010) examined the steady three-dimensional stagnation point flow of a nanofluid past a circular cylinder with sinusoidal radius variation [22]. MHD Mixed Convection Stagnation-Point Flow Over a Stretching Vertical Plate in Porous Medium Filled with a nanofluid in the Presence of Thermal Radiation considered by Eftekhari Yazdi and his colleagues, 2013 [23]. The objective of the present paper is to study the three-dimensional magnetohydrodynamic (MHD) boundary layer of stagnation-point flow in a nanofluid. Using a similarity transform the Navier–Stokes equations have been reduced to a set of nonlinear ordinary differential equations. The resulting nonlinear system has been solved numerically using the Runge–Kutta–Fehlberg method with a shooting technique. The effects of embedded parameters on fluid velocity and temperature have been shown graphically. The case of conventional or regular fluid (φ = 0) with the Prandtl number Pr = 6.2 is also considered for comparison with the results reported by Attia, 2010 [24]. It is found that the comparison shows excellent agreement. It is hoped that the results obtained will not only provide useful information for applications, but also serve as a complement to the previous studies.

## 2. Mathematical formulation of problem

Consider the steady three-dimensional stagnation point flow of a viscous incompressible nanofluid near a stagnation point at a surface coinciding with the plane z = 0, the flow being in a region z > 0. Two equal and opposing forces are applied along the radial direction so that the surface is stretched keeping the origin fixed. We use the cylindrical coordinates *r, φ, z* and assume that the wall is at z = 0, the stagnation point is at the origin and that the flow is in the direction of the negative z-axis. We denote the radial and axial velocity components in frictionless flow by *U* and *W*, respectively, whereas those in viscous flow will be denoted by

*u = u(r, z)* and *w = w(r, z)* where the component in the *φ* direction vanishes. A uniform magnetic field is applied normal to the plate where the induced magnetic field is neglected by assuming very small magnetic Reynolds number. For three-dimensional flow let the fluid far from the plate, as z tends from infinity, be driven by the potential flow; $U = ar$ , $W = -2az$ , where (a > 0) is a constant characterizing the velocity of the mainstream flow [24]. The stretching velocity $u_W(r)$ is assumed to vary linearly from the stagnation point as where c and is positive constants related to the stretching velocity. Under these assumptions and following the nanofluid model proposed by Tiwari and Das [17], the governing equations for the continuity, momentum and energy in laminar incompressible boundary layer flow in a nanofluid can be written as

$$\frac{\partial u}{\partial r}+\frac{u}{r}+\frac{\partial w}{\partial z}=0, \tag{1}$$

$$u\frac{\partial u}{\partial r}+w\frac{\partial u}{\partial z}=U\frac{\partial U}{\partial r}+\nu_{nf}\left[\frac{\partial^2 u}{\partial r^2}+\frac{1}{r}\frac{\partial u}{\partial r}-\frac{u}{r^2}+\frac{\partial^2 u}{\partial z^2}\right]+\frac{\sigma B_0^2}{\rho_{nf}}(U-u) \tag{2}$$

$$u\frac{\partial T}{\partial r}+w\frac{\partial T}{\partial z}=\alpha_{nf}\frac{\partial^2 T}{\partial z^2}, \tag{3}$$

subject to the boundary conditions

$$\begin{aligned} &z=0:\ \ u=cr,\ \ w=0,\ \ T=T_w \\ &z\to\infty:\ \ u=ar,\ \ T\to T_\infty \end{aligned} \tag{4}$$

Here, $T$ is temperature, $\sigma_{nf}$ is the electrical conductivity, $\mu_{nf}$ is the viscosity of the nanofluid, $\alpha_{nf}$ is the thermal diffusivity of the nanofluid and $\rho_{nf}$ is the density of the nanofluid, which are given by Oztop and Abu-Nada, 2008 [25]

$$\mu_{nf}=\frac{\mu_f}{(1-\varphi)^{2.5}},\qquad (\rho)_{nf}=(1-\varphi)(\rho)_f+\varphi(\rho)_s,$$

$$(\rho c_P)_{nf}=(1-\varphi)(\rho c_P)_f+\varphi(\rho c_P)_s, \tag{5}$$

$$\frac{k_{nf}}{k_f}=\frac{\left(k_s+2k_f\right)-2\varphi(k_f-k_s)}{\left(k_s+2k_f\right)+\varphi(k_f-k_s)},\qquad \nu_{nf}=\frac{\mu_{nf}}{\rho_{nf}},$$

where $\varphi$ is the nanoparticle volume fraction, $(\rho c_P)_{nf}$ is the heat capacity of the nanofluid, $k_{nf}$ is the thermal conductivity of the nanofluid, $k_f$ and $k_s$ are the thermal conductivities of the fluid and of the solid fractions, respectively, and $\rho_f$ and $\rho_s$ are the densities of the fluid and of the solid fractions, respectively. To obtain similarity solutions for the system of Eqs. (1)–(3), we introduce the following similarity variables

$$u=crf'(\eta),\quad w=-2\sqrt{c\nu_f}\,f(\eta),\quad \eta=\sqrt{\frac{c}{\nu_f}}\,z,\quad \theta(\eta)=\frac{T-T_\infty}{T_w-T_\infty} \tag{6}$$

Using the non-dimensional variables in Eq. (6), Eqs. (2) and (3) reduce to the following ordinary differential equations

$$f''' + \left\{(1-\phi)^{2.5} M^2\right\}(\varepsilon - f') + (1-\phi)^{2.5}\left(1-\phi+\phi\frac{\rho_s}{\rho_f}\right)\left\{2ff'' + \varepsilon^2 - f'^2\right\} = 0, \tag{7}$$

$$\frac{k_{nf}}{k_f}\theta'' + Pr\left((1-\phi)+\phi\frac{(\rho C_p)_s}{(\rho C_p)_f}\right)f\theta' = 0, \tag{8}$$

and the boundary conditions (4) is become

$$f(0)=0, \quad f'(0)=1, \quad \theta(0)=1,$$
$$f'(\eta)\to\varepsilon = a/c, \quad \theta(\eta)\to 0 \quad as \quad \eta\to\infty, \tag{9}$$

where primes denote differentiation with respect to $\eta$. The Hartman number $M$ , the Prandtl number $Pr$ and the velocity ratio parameter $\varepsilon$ , are, respectively, defined as

$$M^2 = \frac{\sigma B_0^2}{\rho_f a}, \qquad Pr = \frac{\nu_f}{\alpha_f}, \qquad \varepsilon = a/c \tag{10}$$

The physical quantities of interest are the skin friction coefficient $c_f$ and the local Nusselt number $Nu_r$ , which are defined as

$$C_f = \frac{\tau_w}{\rho_f u_w{}^2}, \qquad Nu_x = \frac{rq_w}{k_f(T_w - T_\infty)}, \tag{11}$$

where the surface shear stress $\tau_w$ and the surface heat flux $q_w$ are given by

$$\tau_w = \mu_{nf}\left(\frac{\partial u}{\partial z}\right)_{z=0}, \qquad q_w = -k_{nf}\left(\frac{\partial T}{\partial z}\right)_{z=0}, \tag{12}$$

Using the non-dimensional variables (6), it may be obtained:

$$Re_r^{1/2}C_f = \frac{1}{(1-\varphi)^{2.5}}f''(0), \qquad Nu_r Re_r^{-1/2} = -\frac{k_{nf}}{k_f}\theta'(0) \tag{13}$$

## 3. Results and discussion

Eqs. (7) and (8) subject to the boundary conditions (9) were solved numerically using the Runge–Kutta–Fehlberg method with a shooting technique for some values of the governing parameters. The shown results are for a study on the influences of several non-dimensional parameters. The results of the skin friction coefficient and local Nusselt number as well as the velocity and temperature are illustrated in graphs, while the values of the skin friction coefficient and local Nusselt number for some parameters are given in tables. Three types of nanoparticles: copper (Cu), alumina ($Al_2O_3$), and titania ($TiO_2$) were considered. Following Oztop and Abu-Nada [25] and Bachok, et al., [26], the value of the Prandtl number (Pr) is taken as 6.2 (for water) and the volume fraction of nano particles is from 0 to 0.2 $(0 \le \varphi \le 0.2)$ , in which $\varphi = 0$ corresponds to the regular Newtonian fluid. The thermophysical properties of the fluid and nanoparticles are given in Table 1 [25].

**Table 1.**
Thermophysical properties of the base fluid and the nanoparticles [25].

| Physical properties | Fluid phase (water) | $Cu$ | $Al_2O_3$ | $TiO_2$ |
|---|---|---|---|---|
| $C_p\,(J/kg\,K)$ | 4179 | 385 | 765 | 686.2 |
| $\rho\,(kg/m^3)$ | 997.1 | 8933 | 3970 | 4250 |
| $k\,(W/mK)$ | 0.613 | 400 | 40 | 8.9538 |
| $\alpha\times10^{-7}\,(m^2/s)$ | 1.47 | 1163.1 | 131.7 | 30.7 |

Figs. 1 and 2 show the variation of $f'(\eta)$ and $\theta(\eta)$ for different nanoparticles when . Figs. 3 and 4 respectively show the variations of the velocity profiles $f'(\eta)$ and temperature profiles $\theta(\eta)$ for different nanoparticle volume fractions for copper-water nanofluid.

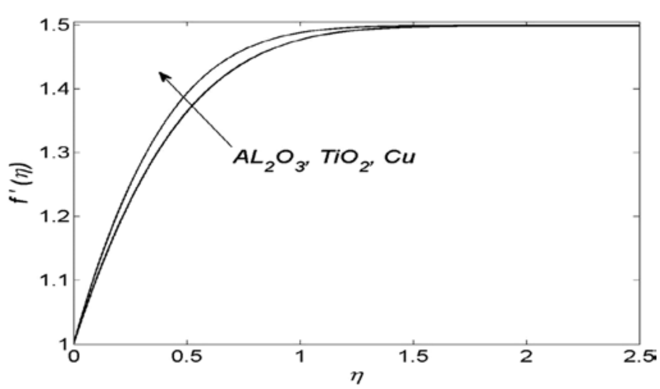


**Fig. 1.** The velocity profiles $f'(\eta)$ for different nanoparticles, when $\varphi=0.1$ .

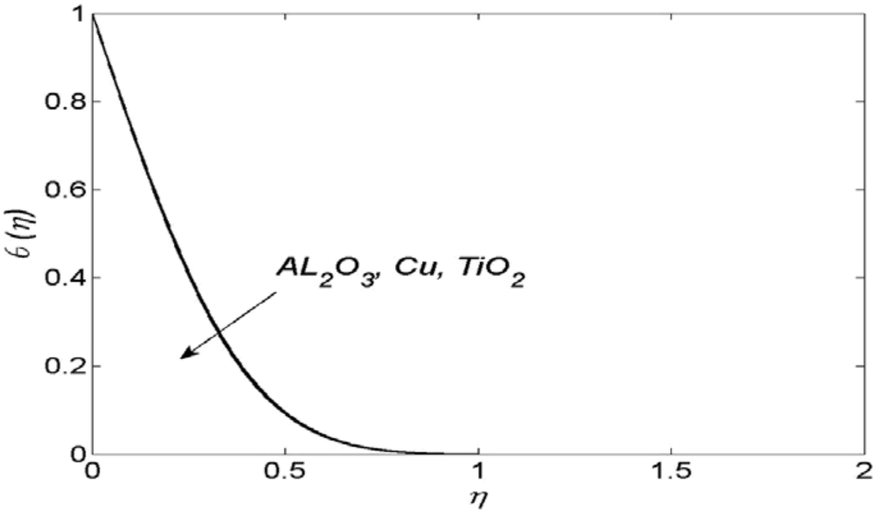


**Fig. 2.** The temperature profiles $\theta(\eta)$ for different nanoparticles, when $\varphi=0.1$ .

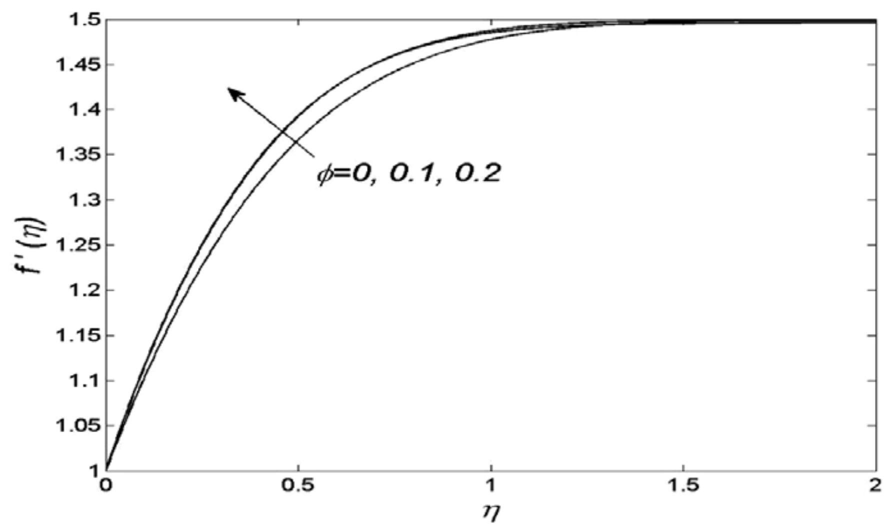


**Fig. 3.** The velocity profile $f'(\eta)$ for different nanoparticle volume fractions $\varphi$ for copper-water nanofluid.

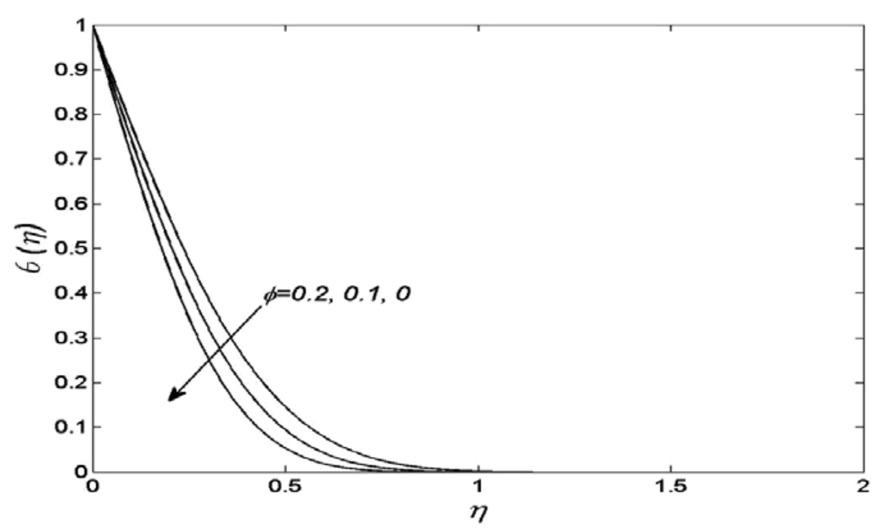


**Fig. 4.** The temperature profiles $\theta(\eta)$ for different nanoparticle volume fractions $\varphi$ for copper-water nanofluid.

It can be seen from Fig. 3 that the velocity components increase with enhancement in the nanoparticle volume fraction parameter ($\varphi$). From Fig. 3, the temperature $\theta$ increases as the nanoparticle volume fraction parameter increases. Fig. 4 shows that the Cu nanoparticle (compared to $Al_2O_3$ and $TiO_2$) has the largest velocities. From Fig. 5, it is observed that the $Al_2O_3$ nanoparticles have the highest value of temperature distribution (compared to Cu and $TiO_2$ ). Fig. 5 is prepared to present the effect of the nanoparticle volume fraction $\varphi$ on the skin friction coefficient $Re_r^{1/2}C_f$ for different types of nanofluids. It is observed that the magnitude of skin friction coefficient increases with the nanoparticle volume fraction $\varphi$. In addition, it is noted that the highest skin friction coefficient is obtained for the Cu anoparticle.

The infuence of the nanoparticle volume fraction $\varphi$ on the local Nusselt number $Nu_r Re_r^{-1/2}$ for different types of nanofluids flows are shown in Fig. 6. It is observed that the local Nusselt number increases with increasing the nanoparticle volume fraction $\varphi$. Moreover, it is noted that the lowest heat transfer rate is obtained for the nanoparticles $TiO_2$ due to domination of conduction mode of heat transfer. This is because $TiO_2$ has the lowest value of thermal conductivity compared to Cu and $Al_2O_3$ , as seen in Table1. However, the difference in the values of Cu and $Al_2O_3$ is negligible. The thermal conductivity of $Al_2O_3$ is approximately one-tenth of that of Cu, as given in Table1. A unique property of $Al_2O_3$ is its slow thermal diffusivity. The reduced value of thermal diffusivity leads to higher temperature gradients and, therefore, higher enhancement in heat transfer. The Cu nanoparticles have high values of thermal diffusivity and, therefore, this reduces the temperature gradients, which will affect the performance of Cu nanoparticles [23].

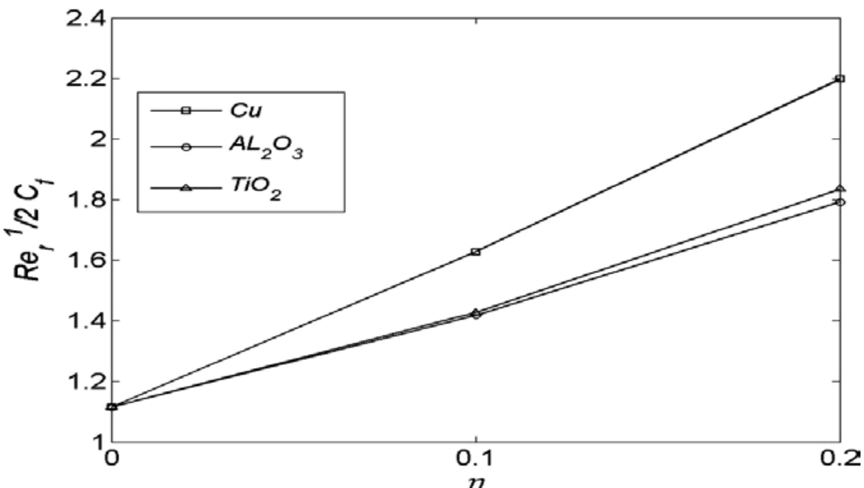


**Fig. 5.** The effect of the nanoparticle volume fraction on the skin friction coefficient for different types of nanofluids.

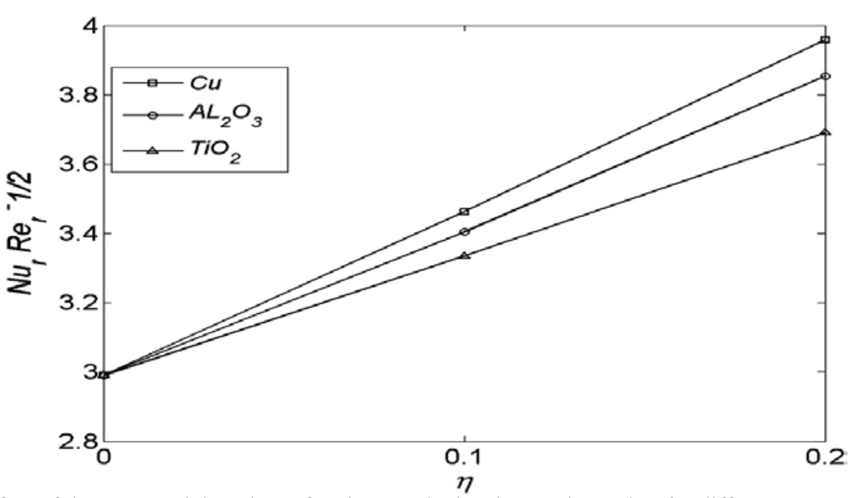


**Fig. 6.** The effect of the nanoparticle volume fraction on the local Nusselt number for different types of nanofluids.

The effect of $M$ on the velocity profiles $f'(\eta)$ and temperature profiles $\theta(\eta)$ for copper-water nanofluid ($\varphi=0.2.$) are illustrated in Figs. 7 and 8 respectively. Fig. 7 displays that the velocity $f'(\eta)$ increases as increases. Moreover, The boundary layer thickness is increased by increasing $M$. From Fig. 8, it can be seen that the temperature profiles $\theta(\eta)$ decrease as M increases. The effect of $\varepsilon$ on the velocity profiles $f'(\eta)$ and temperature profiles $\theta(\eta)$ for copper-water nanofluid ($\varphi=0.1$ ) are illustrated in Figs. 9 and 10, respectively.

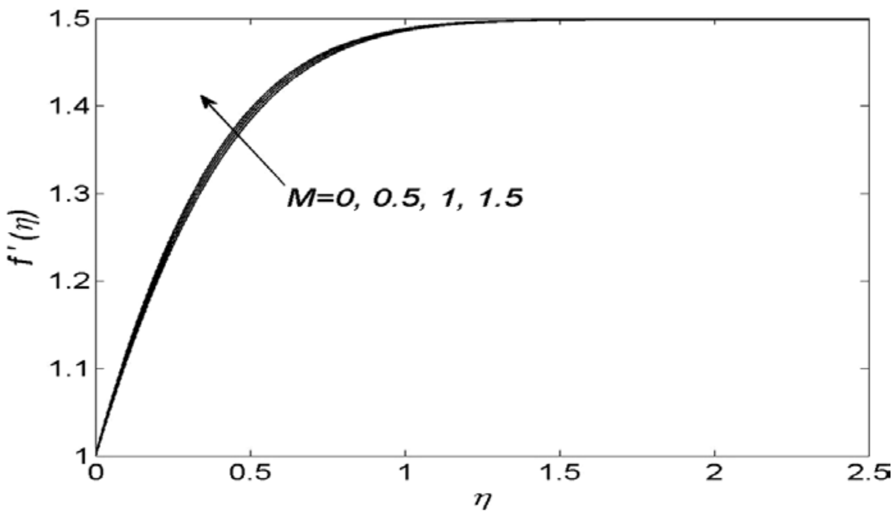


**Fig. 7.** The effect of the Hartman number on the velocity profiles $f'(\eta)$ .

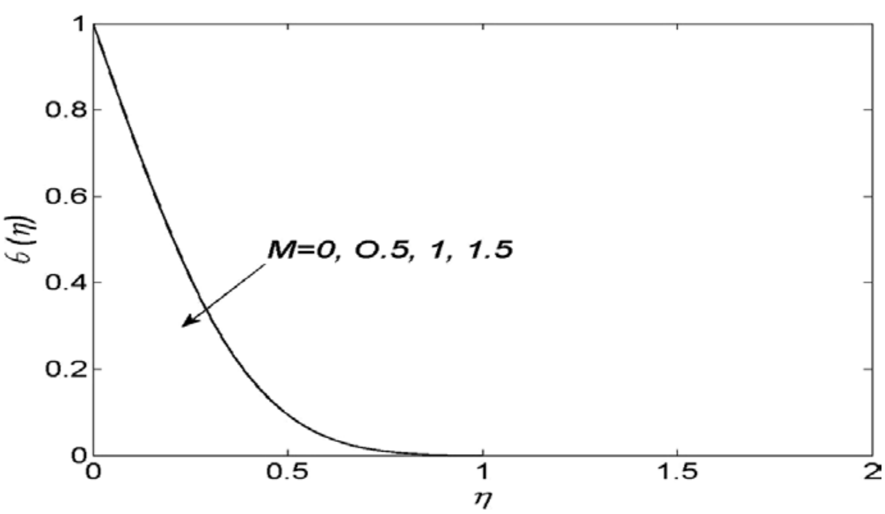


**Fig. 8.** The effect of the Hartman number on the temperature profiles $\theta(\eta)$ .

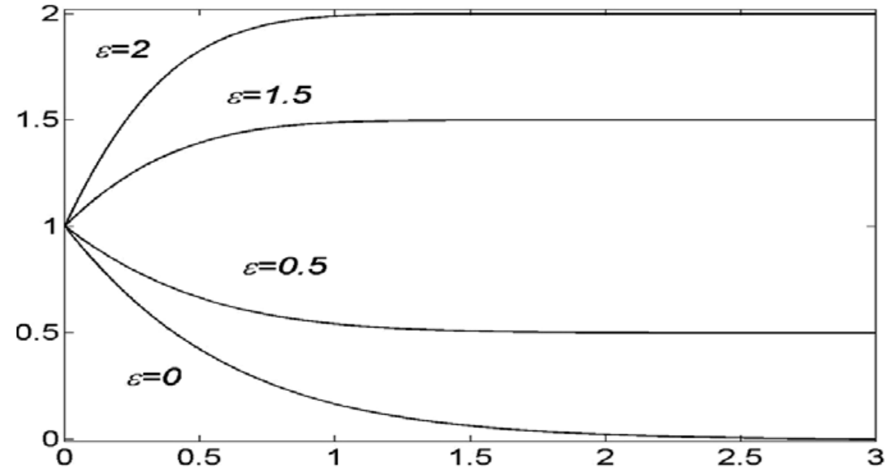


**Fig. 9.** The effect of the velocity ratio parameter $\varepsilon$ on the velocity profiles $f'(\eta)$ for copper-water nanofluid, when $\varphi=0.1$ .

Fig. 9 displays that when $\varepsilon$ >1, the flow has a boundary layer structure and the thickness of the boundary layer decreases with increase in $\varepsilon$ . According to Mahapatra and Gupta (2002) [27], it can be explained as follows: for a fixed value of c corresponding to the stretching of the surface, an increase in a in relation to c (such that $\varepsilon$ >1) implies an increase in straining motion near the stagnation region resulting in increased acceleration of the external stream, and this leads to thinning of the boundary layer with an increase in $\varepsilon$ . Further, it is seen from Fig. 10 that when $\varepsilon$ < 1, the flow has an inverted boundary layer structure. It results from the fact that when $\varepsilon$ < 1, the stretching velocity cx of the surface exceeds the velocity ax of the external stream. From Fig. 10, the temperature $\theta$ decreases as the velocity ratio parameter $\varepsilon$ increases. Fig. 11 shows that the thermal boundary layer thickness increases with decrease in the value of $Pr$ which is associated with an increase in the wall temperature gradient and, hence, produces an increase in the surface heat transfer rate in both the cases of assisting and opposing flows.

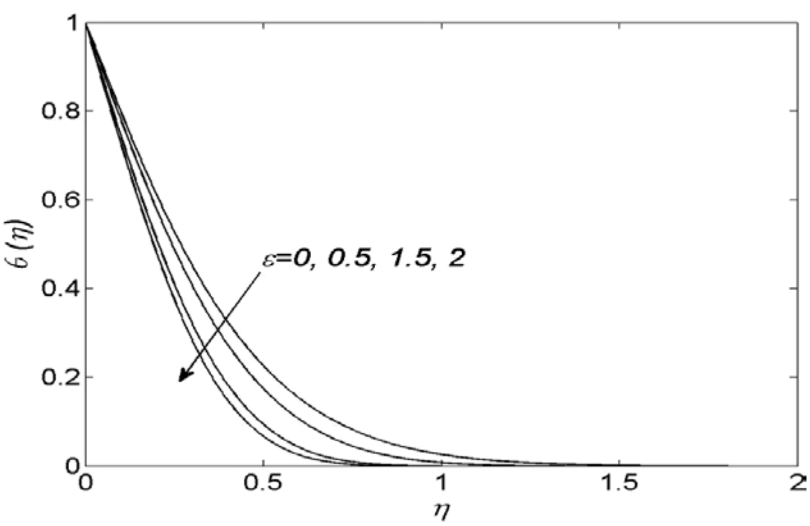


**Fig. 10.** The effect of the velocity ratio parameter $\varepsilon$ on the temperature profiles $\theta(\eta)$ for copper-water nanofluid, when $\varphi=0.1$ .

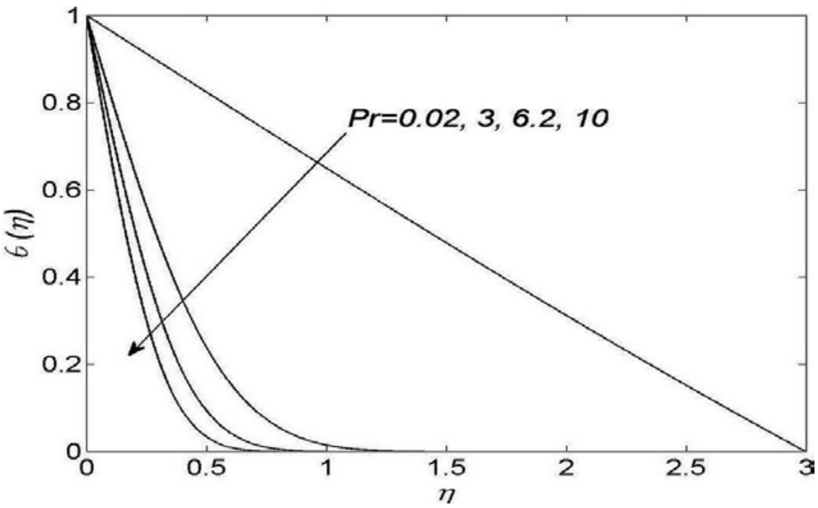


**Fig. 11.** The effect of the Prandtl number $Pr$ on the temperature profiles $\theta(\eta)$ for copper-water nanofluid, when $\varphi=0.1$ .

Further, the temperature θ decreases with the increase in Pr. The effects of thermal buoyancy force are more pronounced on dimensionless temperature for a fluid with a small $Pr$ . For small values of $Pr$ ($<< 1$), the fluid is highly conductive. Physically, if $Pr$ increases, the thermal diffusivity decreases and this phenomenon leads to the decreasing of energy transfer ability that reduces the thermal boundary layer [23]. Table 2 shows the values of the skin friction coefficient $Re_r^{1/2}C_f$ and the local Nusselt number $Nu_rRe_r^{-1/2}$ for some values of the nanoparticle volume fraction $\varphi$ using different nanoparticles. It is observed that, the large values of average Nusselt number and skin friction coefficient can be obtained by adding copper. From Table 2, clearly, the behavior of the present results are in good agreement with the numerical results of Attia [24] for regular fluid ($\varphi = 0$). The values of the skin friction coefficient and the local Nusselt number are tabulated in Table 3 for various values of the Hartman number $M$ , the velocity ratio parameter $\varepsilon$ , the Prandtl number $Pr$. The values of the local Nusselt number increases when enhancement in $M$, $\varepsilon$ and $Pr$. From this table, the magnitude of the skin friction coefficient increases by increasing $M$ and $\varepsilon$ .

**Table 2.**
The effect of the various nanoparticle volume fractions on the local Nusselt number and the skin friction coefficient for the different nanoparticles, when $M = 1$ , $\varepsilon = 1.5$ and $pr = 6.2$ .

| $\varphi$ | Attia [25] | | $Cu$ | | $Al_2O_3$ | | $TiO_2$ | |
|---|---|---|---|---|---|---|---|---|
| | $Re_r^{1/2}C_f$ | $Nu_rRe_r^{-1/2}$ | $Re_r^{1/2}C_f$ | $Nu_rRe_r^{-1/2}$ | $Re_r^{1/2}C_f$ | $Nu_rRe_r^{-1/2}$ | $Re_r^{1/2}C_f$ | $Nu_rRe_r^{-1/2}$ |
| 0.00 | 1.1157 | 2.9902 | 1.11571 | 2.99022 | 1.11571 | 2.99022 | 1.11571 | 2.99022 |
| 0.05 | - | - | 1.36251 | 3.21546 | 1.25325 | 3.18435 | 1.26102 | 3.11415 |
| 0.10 | - | - | 1.62747 | 3.46267 | 1.41914 | 3.40471 | 1.42734 | 3.33459 |
| 015 | - | - | 1.93215 | 3.72324 | 1.61235 | 3.62354 | 1.63214 | 3.50218 |
| 0.20 | - | - | 2.19825 | 3.95888 | 1.79196 | 3.85410 | 1.83549 | 3.69083 |

**Table 3.**
The effect of $M$, $\varepsilon$ and $Pr$ on local Nusselt number and skin friction coefficient for copper-water nanofluid, when $\varphi=0.1$.

| $M$ | $\varepsilon$ | Pr | $Re_x^{1/2}C_f$ | $Nu_x Re_x^{-1/2}$ |
|---|---|---|---|---|
| 0.0 | 1.5 | 6.2 | 1.52672 | 3.45388 |
| 0.5 | | | 1.57776 | 3.45827 |
| 1 | | | 1.62737 | 3.46267 |
| 1.5 | | | 1.67541 | 3.46666 |
| 1 | 0.0 | 6.2 | -2.12226 | 2.72714 |
| | 0.5 | | -1.28247 | 2.96716 |
| | 1.5 | | 1.62737 | 3.46267 |
| | 2 | | 3.55810 | 3.69523 |
| 1 | 1.5 | 0.03 | 1.62737 | 0.46940 |
| | | 3 | 1.62737 | 2.45274 |
| | | 6.2 | 1.62737 | 3.46267 |
| | | 10 | 1.62737 | 4.35004 |

## 5. Conclusions

Here, the steady three-dimensional laminar flow of a viscous nanofluid past a plate in the presence of magnetic field was investigated. The governing partial differential equations were converted to ordinary differential equations using a suitable similarity transformation and then were solved numerically using the Runge–Kutta–Fehlberg method with a shooting technique. Similarity solution was presented which depended on the nanoparticle volume fraction parameter $\varphi$, the Hartman number $M$, the Prandtl number $Pr$ on the flow and heat transfer characteristics. Finally, from the presented analysis, the following observations are noted.

- For all three nonoparticles, the magnitude of the skin friction coefficient and local Nusselt number increases with increasing the nanoparticle volume fraction $\varphi$ for both cases of buoyant assisting and opposing flows.
- For a fixed value of the nanoparticle volume fraction $\varphi$, the velocity of fluid increases by increasing $M$ and $\varepsilon$.
- For a fixed value of the nanoparticle volume fraction $\varphi$, the temperature increases when $M$, $\varepsilon$ and $Pr$ decreases.
- The volume fraction of nanoparticles is a key parameter for studying the effect of nanoparticles on flow fields and temperature distributions.
- The type of nanofluid is a key factor for heat transfer enhancement. The highest values were obtained when Cu nanoparticles was used.
- The highest values of the skin friction coefficient and the local Nusselt number were obtained for the Cu nanoparticles compared to $Al_2O_3$ and $TiO_2$.

## References

[1] K. Hiemenz, Die Grenzschicht an einem in den gleichformingen Flussigkeitsstrom einge-tauchten graden Kreiszylinder, Dingl. Polytech. J. 326 (1911) 321–324.

[2] F. Homann, Der Einfluss grosser Zahigkeit bei der Stromung um den Zylinder und um die Kugel, Z. Angew. Math. Mech. 16 (1936) 153–164.

[3] E. R. G. Eckert, Die berechnung des wärmeübergangs in der laminaren grenzschicht umströmter körper, VDI Forschungsheft, (1942) 416.

[4] S. Dinarvand, On explicit, purely analytic solutions of off-centered stagnation flow towards a rotating disc by means of HAM, Nonlinear Anal. Real World Appl.11 (2010) 3389–3398.

[5] H. M. Duwairi, R. A. Damseh, Magnetohydrodynamic natural convection heat transfer from radiate vertical porous surfaces, Heat Mass Trans., 40 (2004) 787–92.

[6] H. M. Duwairi, R. A. Damseh. MHD-buoyancy aiding and opposing flows with viscous dissipation effects from radiate vertical surfaces, Can. J. Chem. Eng, 82 (2004) 613–618.

[7] M.C. Ece, Free convection flow about a cone under mixed thermal boundary conditions and a magnetic field, Appl. Math. Model. 29 (2005) 1121–1134.

[8] S. Dinarvand, A. Doosthoseini, E. Doosthoseini, M. M. Rashidi , Series solutions for unsteady laminar MHD flow near forward stagnation point of an impulsively rotating and translating sphere in presence of buoyancy forces, Nonlinear Anal. Real World Appl. 11 (2010) 1159–1169.

[9] S. Dinarvand, The laminar free-convection boundary-layer flow about a heated and rotating down-pointing vertical cone in the presence of a transverse magnetic field, Int. J. Numer. Meth. Fluids, 67 (2011) 2141–2156

[10] S.U.S. Choi, Enhancing thermal conductivity of fluids with nanoparticle, in: D.A. Siginer, H.P. Wang (Eds.), Developments and Applications of Non- Newtonian Flows, ASME FED, 66 (1995) 99–105.

[11] S.U.S. Choi, Z.G. Zhang, W. Yu, F.E. Lock

wood, E.A. Grulke, Anomalously thermal conductivity enhancement in nanotube suspensions, Appl. Phys. Lett. 79 (2001) 2252–2254.

[12] H. Kang, S. H. Kim, J. M.Oh, Estimation of Thermal Conductivity of Nanofluid using Experimental Effective Particle Volume, Exp. Heat Transf., 19 (2006) 181–191.

[13] V. Velagapudi, R. K. Konijeti, C. S. K. Aduru, Empirical Correlation to Predict Thermophysical and Heat Transfer Characteristics of Nanofluids, Therm. Scien., 12 (2008) 27–37.

[14] A.Turgut, et al., Thermal Conductivity and Viscosity Measurements of Water-Based TiO2 Nanofluids, Int. J. Thermophys, 30 (2009) 1213–1226.

[15] V. Y. Rudyak, A. A. Belkin, E. A.Tomilina, On the Thermal Conductivity of Nanofluids, Technic. Phys. Lett., 36 (2010) 660–662.

[16] C. Murugesan, S. Sivan, Limits for Thermal Conductivity of Nanofluids, Therm. Scie., 14 (2010) 65–71.

[17] R.J. Tiwari, M.K. Das, Heat transfer augmentation in two-sided lid-driven differentially heated square cavity utilizing nanofluids, Int. J. Heat Mass Transfer, 50 (2007) 2002–2018.

[18] A. K. Nayak, R. K. Singh, P. P. Kulkarni, Measurement of Volumetric Thermal Expansion Coefficient of Various Nanofluids, Tech. Phys. Lett., 36 (2010) 696–698.

[19] S. Ahmad, I. Pop, Mixed convection boundary layer flow from a vertical flat plate embedded in a porous medium filled with nanofluids, Int. Comm. Heat Mass Transfer, 37 (2010) 987–991.

[20] S. Dinarvand, A. Abbassi, R. Hosseini, I. Pop, homotopy analysis method for mixed convective boundary layer flow of a nanofluid over a vertical circular cylinder, Therm. Scien., 19 (2015) 549-556.

[21] J.A. Gbadeyan, M.A. Olanrewaju, P.O. Olanrewaju, Boundary Layer Flow of a Nanofluid Past a Stretching Sheet with a Convective Boundary Condition in the Presence of Magnetic Field and Thermal Radiation, Austral. J. Bas. and Appl. Scie., 5 (2011) 1323–1334.

[22] S. Dinarvand, R. Hosseini, E. Damangir, I. Pop, Series solutions for steady three-dimensional stagnation point flow of a nanofluid past a circular cylinder with sinusoidal radius variation, Meccanica, 48 (2013) 643-652.

[23] M. Eftekhari Yazdi, A. Moradi, S. Dinarvand. MHD Mixed Convection Stagnation-Point Flow Over a Stretching Vertical Plate in Porous Medium Filled with a Nanofluid in the Presence of Thermal Radiation, Arab J Sci Eng. 39 (2013) 2251-2259.

[24] H.A. Attia, Steady three dimensional hydromagnetic stagnation point flow towards a stretching sheet with heat generation, Italian J Pure App Math, 27 (2010) 9-18.

[25] H.F. Oztop, E. Abu-Nada, Numerical study of natural convection in partially heated rectangular enclosures filled with nanofluids, Int. J. Heat & Fluid Flow, 29 (2008) 1326–1336.

[26] N. Bachok, A. Ishak, R. Nazar, I. Pop, Flow and heat transfer at a general three-dimensional stagnation point in a nanofluid, Physica B, 405 (2010) 4914–4918.

[27] T.R. Mahapatra, A.S. Gupta, Heat transfer in stagnation-point towards a stretching sheet, Heat Mass Transf., 38 (2002) 517–521.